Status of the Southern African Large Telescope (SALT) First-Generation Instruments

D. A. H. Buckley[*a], E. B. Burgh[†b], P. L. Cottrell[‡c], K. H. Nordsieck[§b], D. O'Donoghue[**a] and T. B. Williams[††d]

[a]South African Astronomical Observatory, Observatory, Cape Town, South Africa
[b]Space Astronomy Lab, University of Wisconsin, Madison, Wisconsin, USA
[c] Department of Physics and Astronomy, University of Canterbury, Christchurch, New Zealand
[d] Department of Physics and Astronomy, Rutgers University, Piscataway, USA

ABSTRACT

"First light" of the Southern African Large Telescope was declared on 1 Sep 2005 and the first scientific programs have now begun. This paper discusses the completion and commissioning of the first-light instruments: the UV-visible imaging camera, SALTICAM, and the prime focus imaging spectrograph, the Robert Stobie Spectrograph (RSS). The innovative aspects and tight constraints on the design of these prime focus instruments are described, as well as the first scientific results. These instruments, which are all seeing limited, operate in the UV-visible region (320 – 900 nm), and will provide capabilities for broad and narrow band imaging, long-slit and multi-object spectroscopy (R ~ 6000 for seeing limit), spectropolarimetry and Fabry-Perot imaging spectroscopy (R ~ 320–9,000). Time resolved studies are an important aspect of the overall SALT science drivers and special efforts were made to ensure an ability to run at ~10 Hz, with minimal dead time, by employing frame transfer CCDs. Finally, we present the design and status of the fiber-fed high resolution échelle spectrograph, SALTHRS, the last of the "first generation" SALT instruments.

Keywords: Astronomical instruments, spectrographs, imaging camera, VPH gratings, polarimetry, Fabry-Perot spectroscopy, science drivers, high speed astronomy

1. INTRODUCTION

In mid-2005, construction of the Southern African Large Telescope (SALT)[1,2,3,4] and its first two "first-light" instruments was completed, having taken 5½ years since the project began. It then entered an intensive period of commissioning (telescope and instruments), expected to last until late-2006. The culmination of activities in 2005 was the official inauguration of SALT by the President of South Africa, Thabo Mbeki, on 10 November. This had been preceded by the declaration on 1 September of "first light", defined as full science-field (8 arecmin diameter) images taken with the complete array of 91 mirror segments, exactly 5 years after the ground-breaking ceremony.

Although the basic design of SALT was similar to that of the Hobby-Eberly Telescope (HET)[5,6], there were significant departures brought about to enhance performance and take advantage of the lessons learned with the HET. Almost every subsystem on SALT has been redesigned resulting in expected improvements in performance. These design changes have given SALT new scientific capabilities, particularly regarding the enhanced UV/blue throughput and the ability to mount larger and more massive instrumentation at the prime focus. The major effects of these design changes are itemized here:

[*] dibnob@saao.ac.za; SAAO, PO Box 9, Observatory 7935, South Africa; phone +27 21 4606286; fax +27 21 4473639;
[†] ebb@sal.wisc.edu; Space Astronomy Laboratory, University of Wisconsin-Madison, WI 53706, USA;
[‡] peter.cottrell@canterbury.ac.nz; University of Canterbury, Private Bag 4800, Christchurch 8020, New Zealand
[§] khn@sal.wisc.edu; Space Astronomy Laboratory, University of Wisconsin-Madison, WI 53706, USA;
[**] dod@saao.ac.za; SAAO, PO Box 9, Observatory 7935, South Africa; phone +27 21 4606286; fax +27 21 4473639;
[††] williams@physics.rutgers.edu; Dept. of Physics and Astronomy, Rutgers University, Piscataway, NJ 08854-8019, USA.

1. A redesigned spherical aberration corrector (SAC)[7], which gave a larger field of view (8 arcmin diameter), improved imaging quality (EE50 < 0.2 arcsec), a larger entrance pupil (11-m diameter) and, consequently, a ~15% increase in light collection. These improvements have led to the development of imaging instruments on SALT (e.g. SALTICAM, RSS imaging).
2. By using multi-layer protected Ag/Al coatings[8] on the four mirrors, sensitivity at short wavelengths have been enhanced, allowing observations down to the atmospheric cut-off at 320 nm (see Figure 1).
3. Active primary mirror and prime focus payload alignment system, including capacitive edge sensors on the former and laser auto-collimator and a Mach-Zender distance measuring interferometer on the latter. This is expected to improve image quality retention.
4. A greatly enhanced Prime Focus Payload with 4 focal stations, and including a sensitive science grade acquisition camera (SALTICAM), separate focus and auto-guiding cameras, a facility atmospheric dispersion corrector, a moving exit pupil baffle and calibration system for flat-fields and arcs.

The set of first-light instruments[9,10] were therefore designed to take full advantage of the expected improvements in telescope image quality, the larger science field of view (8 arcmin diameter) and good UV/blue response.

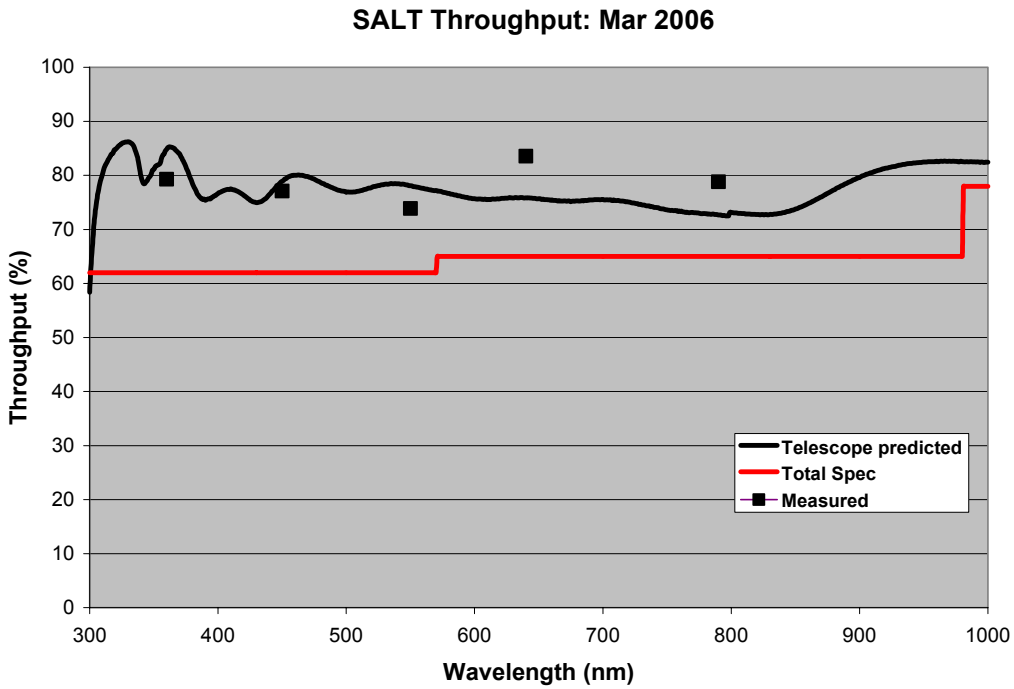

Figure 1: The total throughput (reflectance) measurements of all five SALT mirrors (primary plus four reflections of the SAC) determined from UBVRI imaging with SALTICAM (squares) compared to the predicted performance and the minimum specification.

2. SALT SCIENCE COMPETIVENESS

For a telescope like the SALT, one has to consider how they can be competitive with more versatile, and usually better funded, telescopes of similar aperture. Clearly without having a phased primary mirror array, such a telescope will never be competitive in terms of imaging capability. This is why the HET was conceived as a purely "Spectroscopic Survey Telescope"[5], operating in the visible region. Despite the design constraints of SALT and HET, these telescopes are competitive in many areas. One should also not lose sight of the advantage such telescopes have in the amount of 10-m telescope time available for a given project. The smaller user communities benefit from better access compared, for example, to a national facility with a much larger over-subscription rate. Often important science programs are impossible to do because of the difficulty in securing enough, and regular, observing time, particularly for time-variable

astrophysical phenomena. So there can be a tendency for projects to become shorter timescale, less encompassing or less ambitious. Consequently, certain types of observations are under-represented on large telescopes, despite the great promise that these have in opening up new 'phase space' of astrophysical inquiry. Examples here include:

- spectroscopy down to the atmospheric UV cutoff
- polarimetry (linear and circular)
- high-speed spectroscopy and photometry
- synoptic observations over a range of timescales (days to years).

These have become important considerations when deciding on the science programs best suited to SALT. They have also guided the development of the SALT design and the choice of an initial instrument suite. In addition, the restrictions imposed by the SALT design must also guide the science drivers and hence the choice of instruments. SALT is ideally suited to science programs for which one or more of the following criteria apply:

- Objects are confined to the Declination limit $+10^{\circ} \geq \delta \geq -75^{\circ}$
- High spatial resolution is not required (telescope error budget is EE50=0.6 arcsec)
- Observation limited to wavelengths of ~320 nm $\leq \lambda \leq$ ~900 nm for first-generation instruments, possibly extending to 2.5μm for second generation instruments.
- Objects are uniformly distributed on the sky with densities of $<$ a few degree^{-2} or $<$ a few arcmin^{-2}, respectively, depending on observing mode. The lower density is derived from the requirement of no azimuth movement between observations of a single program, to maximize efficiency. The higher number comes from the expected performance of multi-object spectroscopy in the 8 arcmin science FoV with RSS.
- Time resolved studies of objects will be on timescales, τ, of either ~100 ms $<\tau<$ ~a few hours, or $\tau >$ a day

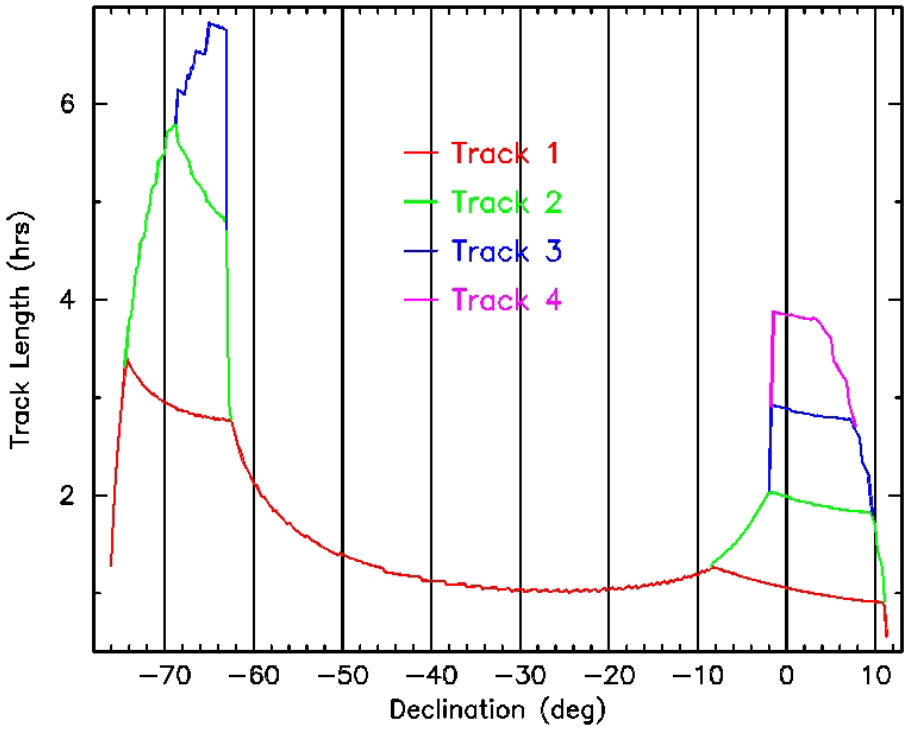

Figure 2: Potential SALT total observation times. The lower curve (Track 1) assumes the azimuth is chosen to ensure the earliest acquisition of a target in the east, which is then tracked until it leaves the visibility annulus. The remaining tracks are the gains made when allowing for successive azimuth moves to the West, where appropriate, where Track 2 is for one additional azimuth move, Track 3 for two moves and Track 4 for three moves.

With the advent of the redesigned SAC[7] giving SALT a respectable science field of 8 arcmin diameter, the imaging capability has been exploited, initially with the broadband visible camera, SALTICAM. The spectroscopic capabilities of SALT have initially been confined to the visible domain (320 – 900 nm), although an upgrade path to support near IR spectroscopy, to between 1.4 and 1.9μm, is being planned.

SALT's primary mirror array of 91 × 1 meter (edge to edge) segments, 11 meters from corner to corner, gives a maximum effective collecting area of ~60 meter^2. This is for an effective 11-m diameter entrance pupil produced by the SAC and includes the effect of all mirror gaps, shadowing, SAC central obstruction, etc. This is equivalent to an unobstructed ~9-m diameter mirror. Such a large area of the primary mirror will give SALT the capability of observing very faint astronomical objects (to R ~ 28 at lowest spectral resolutions) for periods of ~1-3 hours at a time.

When discussing potential science programs, it is instructive to consider the sky visibility of SALT and the total tracking time available at different declinations (Figure 2). This plot emphasizes the importance of concentrating on southern objects (e.g. the Magellanic Clouds). Total track times are determined by the ± 6° range which the tracker has, plus the maximum tip/tilt of the payload hexapod legs, which is 8.5°. Of course the telescope is capable of extending the observing times on a particular target if the whole structure is lifted and rotated in azimuth to the west. Targets can also potentially be observed for extended periods, twice a night, depending on their position, as they rise in the east, and later, when they set in the west.

3. SALT'S FIRST-GENERATION INSTRUMENTS

Initial plans were to fund three first-generation science instruments from the SALT construction budget[9], through a combination of both cash and "in-kind" funding from SALT consortium partners. These three instruments were:

1. SALTICAM, a broad-band imaging camera
2. RSS, the Robert Stobie Spectrograph, formerly known as the Prime Focus Imaging Spectrograph (PFIS)
3. SALTHRS, a fibre fed high resolution échelle spectrograph, primarily designed for single objects.

All three instruments were to be built by SALT consortium members, but by the time SALT was completed in 2005, only two of these instruments (SALTICAM and RSS) were built and installed on the telescope. Both are now referred to as the SALT "first light" instruments. The third instrument, SALTHRS, has had both technical and funding difficulties, which have caused a delay in its development. The status of this instrument will be reported later.

All three first-generation instruments were designed to be seeing-limited (where the zenith median site seeing in the V-band is 0.9 arcsec FWHM) and will operate over the UV-visible band from 320 to 900 nm (SALTHRS is currently designed to operate over 370 – 890 nm). SALTICAM and RSS are both mounted at prime focus, thus taking full advantage of the good UV/blue performance afforded by the high efficiency SAC mirror coatings. The following sections discuss the designs of these instruments.

4. SALTICAM: SALT IMAGING CAMERA

SALTICAM was built at the South African Astronomical Observatory (SAAO), where Dr Darragh O'Donoghue was the Principal Investigator. This instrument was conceived as a multi-purpose device, capable of performing roles as both an efficient acquisition camera and a scientific imaging photometer[10,12]. SALTICAM was built in two stages, the first without the eventual focal reduction optics, when it served the purpose of the SALT Verification Instrument (VI), used to undertake initial on-sky testing of the telescope. This configuration consisted just of the cryostat containing a mosaic of two E2V CCD 44-82 chips, plus a filter wheel, both mounted on an X-Y translation stage at the straight-through prime focus position on SALT, which was eventually occupied by RSS. Here it was used to commission SALT and perform various acceptance tests.

SALTICAM VI was completed in September 2003, and was used for the first on-sky tests, including acquisition, tracking and guidance observations, and throughput tests. In the January 2005 SALTICAM VI was removed from the telescope and underwent its transformation from VI mode to the so-called Acquisition Camera and Science Imager (ACSI) mode, in which focal reducing fore-optics were mounted. In July 2005 SALTICAM was installed at its final position, at one of the prime foci, fed by a 45° mirror. The fore-optics provide focal reduction (from f/4.2 to f/2) enabling a more suitable plate scale and allowing for the entire 8 arcmin diameter science field and the surrounding 1 arcmin wide guidance annulus to be imaged onto the mosaiced 4K × 4K detector area (i.e. a field of ~10 × 10 arcmin). The current filter set available is UBVRcIc, although there are plans to procure both Strömgren and SLOAN filter sets in the near future.

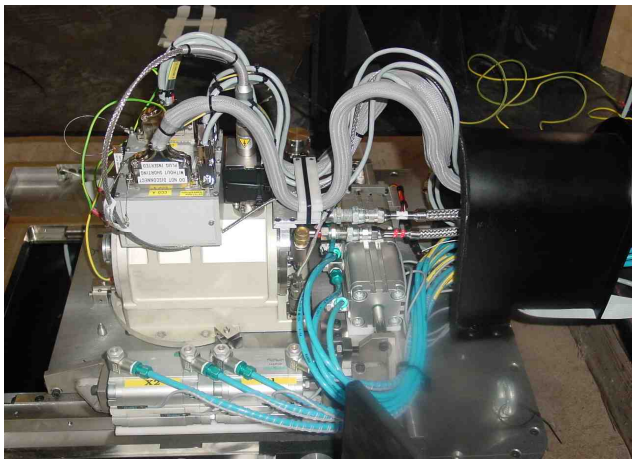

Figure 3: SALTICAM VI, as it looked at the SALT prime focus mounted on a pneumatic X-Y slide.

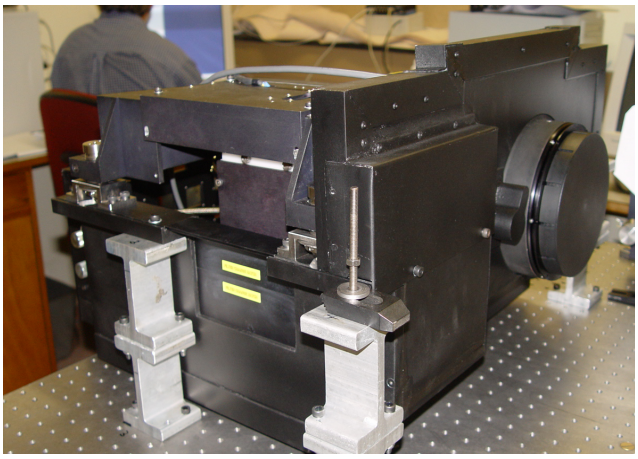

Figure 4: SALTICAM ACSI, undergoing acceptance testing in the lab. The lens barrel is seen to the right with a lens cap on.

5. HIGH TIME RESOLUTION OBSERVATION MODES

SALTICAM and RSS employ the same frame transfer CCDs, which allows for fast acquisition and imaging, in the region 10-20 Hz, with minimal (few ms) dead-time[13]. RSS and SALTICAM will extend the domain of time variability studies on 10-m class telescopes. SALTICAM's optics are designed to allow observations to the UV atmospheric cut off. Although SALT suffers from a varying, under-filled and segmented pupil, it was nonetheless expected that high frequency stochastic variations in effective collecting area would be at a level of < 0.1%, making SALTICAM easily capable of accurate differential photometry, which has already been proven (see Figure 5 for a high-speed differential light curve, sampled at 100 ms). However, careful calibrations using frame standards will be needed for absolute photometry.

Figure 6 illustrates the methods employed for high-time resolution observations with SALTICAM and RSS[13]. For the former, where there is no intermediate focus, an occulting mask, inside the cryostat, can be moved into three different positions, namely:

1. completely removed, for full-frame CCD imaging
2. partially inserted, to block off half of the CCD (storage array) in frame transfer mode, or
3. fully inserted, when a slot is placed at the frame transfer boundary (i.e. between the image and store arrays).

The latter allows just a small region of the CCD to be illuminated, and then row-shifted into the storage array, before beginning another exposure. A target object, and local comparison star(s), can then be placed in the slot to allow for high-speed differential photometry. For RSS a similar mask can be inserted in the telescope's focal plane, where the spectrograph slit is placed, and this can be used to undertake high-speed spectroscopy. In this case a comparison star would be placed along the slit, orthogonal to the slot direction, allowing for the simultaneous observation of spectra from the varying source and a constant comparison.

Predictions for the how fast SALTICAM and RSS can run have been made based on the CCD characteristics[13], and these have subsequently been verified by commissioning observations. For frame transfer mode, with 2 x 2 binning, the shortest exposures are ~2.5 sec, whereas for slot mode, with 64 spatial pixels (~9 arcsec), the shortest exposure possible is ~80 ms.

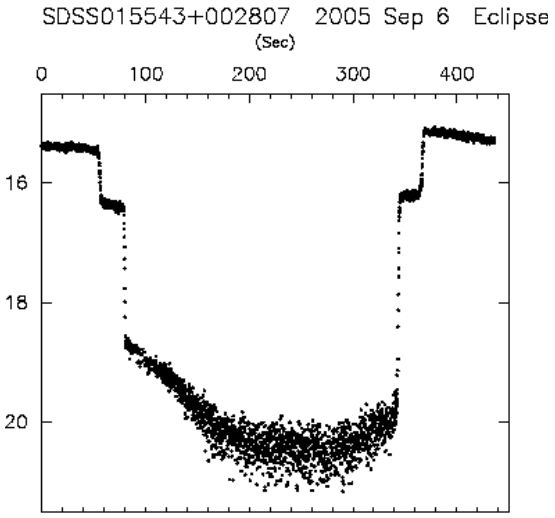

Figure 5: An eclipse light curve of a magnetic CV taken with SALTICAM with 100ms sampling. The steps are due to progressive disappearance and reappearance of accretion hot-spots near the magnetic poles of a white dwarf.

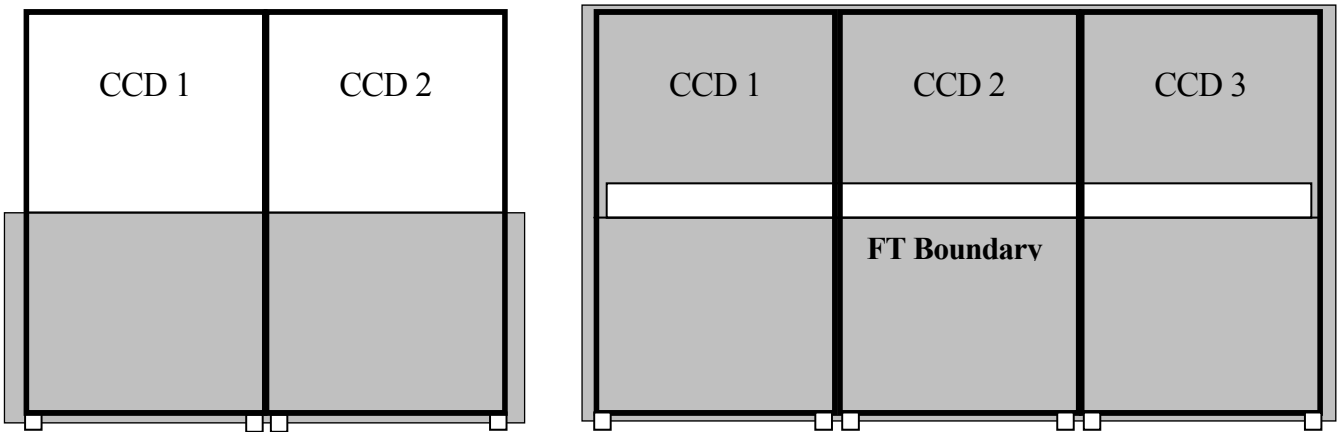

Figure 6: Mosaic layout for SALTICAM (left) and RSS (right) detectors. The large rectangles represent CCD chips, the small boxes at the bottom of each chip represent readout amplifiers. Masks used for the high-speed modes are also shown, the left one demonstrating the SALTICAM frame transfer mask, and the right being the RSS slot mode mask[13].

6. RSS: THE ROBERT STOBIE SPECTROGRAPH

This instrument, which began life as the Prime Focus Imaging Spectrograph (PFIS), was named in memory of Dr Robert S. Stobie, one of the founders of SALT, and past Director of the SAAO. It was installed on SALT in October 2005, and will become the initial work-horse instrument. RSS was built at the University of Wisconsin-Madison, where the Principal Investigator was Professor Ken Nordsieck and the Instrument Scientist Dr. Eric Burgh. Two other SALT partners were also involved in building RSS: Rutgers University (under Professor Ted Williams) were responsible for the Fabry-Perot subsystem and the Invar structure, while the SAAO, under the direction of Dr Darragh O'Donoghue, built the RSS CCD detector system.

RSS resides at the direct prime focus, where it takes advantage of the direct access to the focal plane, and was designed to have a range of capabilities and observing modes, each one remotely and rapidly reconfigurable[10,14,15]. In keeping with the overall philosophy of exploiting the niche areas where SALT has a competitive edge, the instrument has several unique, or rare, capabilities, some afforded by various enabling technologies. These capabilities include:

- The ability to observe down to the UV atmospheric cut-off, at ~320 nm. This is achieved by the judicious use of UV transmitting materials in the optical design, including fused silica, fused quartz, CaF_2 and NaCl (the latter used as central elements in sealed triplets). High throughput has demanded the use of efficient anti-reflection coatings, including Solgel on interior (sealed) lens surfaces[14].
- A fully articulating camera/detector used with Volume Phase Holographic transmission gratings (VPHGs). This, to our knowledge, is only the second spectrograph so designed to take full advantage of VPHGs with varying incidence angle and full articulation (the other being the Goodman Spectrograph on SOAR).
- All Stokes mode spectropolarimetry and imaging polarimetry using either one or both ½ and ¼ waveplate retarders and a large Wollaston beam-splitter mosaic, giving two completely off-set O- and E-images on the detector[16]. High-speed and simultaneous modes will also be available, which is particularly pertinent for time varying polarized sources.
- Fabry-Perot imaging spectroscopy in the range 430-860 nm using three etalons, in dual mode for medium and high resolution, providing three resolution regimes of R = 320–770, 1250– 1650 and 9000.
- the use of fast frame-transfer CCDs allowing for high-speed observations in all observing modes.

In addition, RSS is also be capable of:

- Wavelength coverage from ~320 nm to 900 nm, including the provision of an upgrade path for a near IR arm (to between 1.4 and 1.7 microns) using a dichroic beamsplitter.
- Low to medium resolution spectroscopy (up to R ~ 5500 with 1 arcsec slits; R ~ 10000 with 0.6 arcsec slits) using efficient and tuneable VPH gratings.
- Multiple object spectroscopy (MOS) using laser cut graphite focal plane slit masks, of up to ~100 objects at a time. A "nod and shuffle" mode will also be employed for accurate background subtraction.
- Narrowband imaging.

Figure 7 shows the optical design of RSS and the arrangements for imaging, Fabry-Perot imaging spectroscopy and grating spectroscopy. For the latter, VPH transmission gratings are inserted in the collimated beam, and rotated to specific incidence angles, which determine both the wavelength and resolution. The camera and detector then have to rotate twice this angle to capture the optimally Bragg diffracted orders, this requires an accurate articulation of the whole camera-detector unit by up to 100º (for a 50º incidence angle). More detailed discussions of the optical design and the various operational modes of RSS are available elsewhere[14,15].

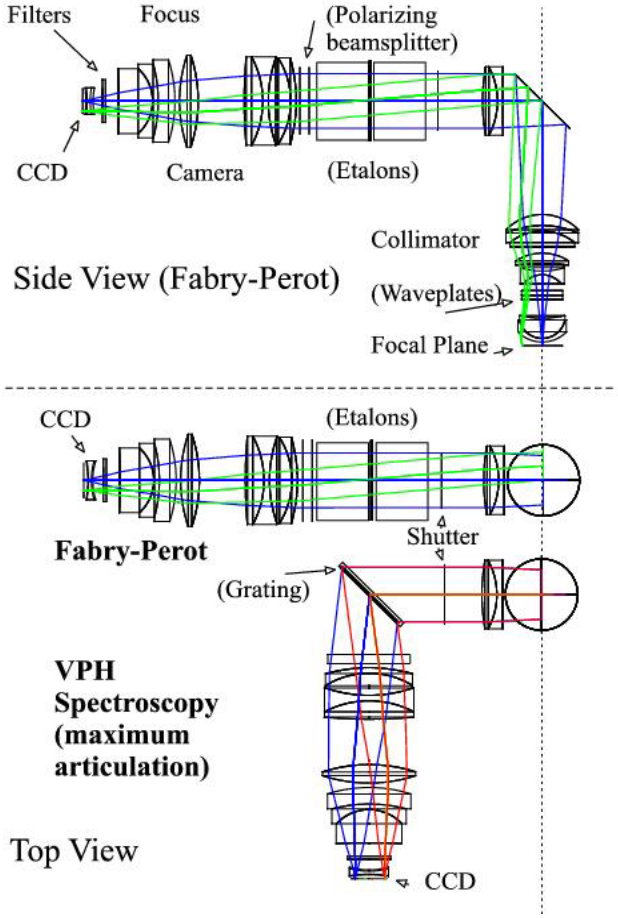

Figure 7: The optical layout of RSS. Both a top and side view are shown with the spectrograph in imaging/F-P configuration as well as nearly fully articulated for VPH spectroscopy.

6.1 RSS CCD Detector

The CCDs for RSS (and SALTICAM) are E2V CCD 44-82 chips, each with 2K × 4K × 15 micron pixels. A mosaic of CCD chips (2 or 3, respectively, for SALTICAM and RSS) are housed in an evacuated cryostat and thermally connected to the cold end of a CryoTiger closed-cycle cooler, which cools the chips sufficiently to render dark current insignificant while minimizing QE reduction. The detectors are managed by an SDSU III CCD controllers[13].

These CCDs are thinned, back-illuminated deep depletion devices, coated for good UV response. They were designed to run in frame transfer mode for high time resolution, which should allow for observations at ~10Hz for high-speed spectroscopy or spectropolarimetry, with insignificant readout time losses. An example of the how high-speed spectroscopy mode operates is shown in Figure 8. Three of these chips were mosaiced together for RSS, i.e. an effective 4K × 6K detector area, although binning by at least 2 × 2 will be usual for most situations (1 unbinned pixel = 0.13 arcsec). All the chips are cosmetic Grade 0 devices with low readout noise (2.0-2.4 e) and excellent QE (one of the chips has a QE of 80% at 350 nm).

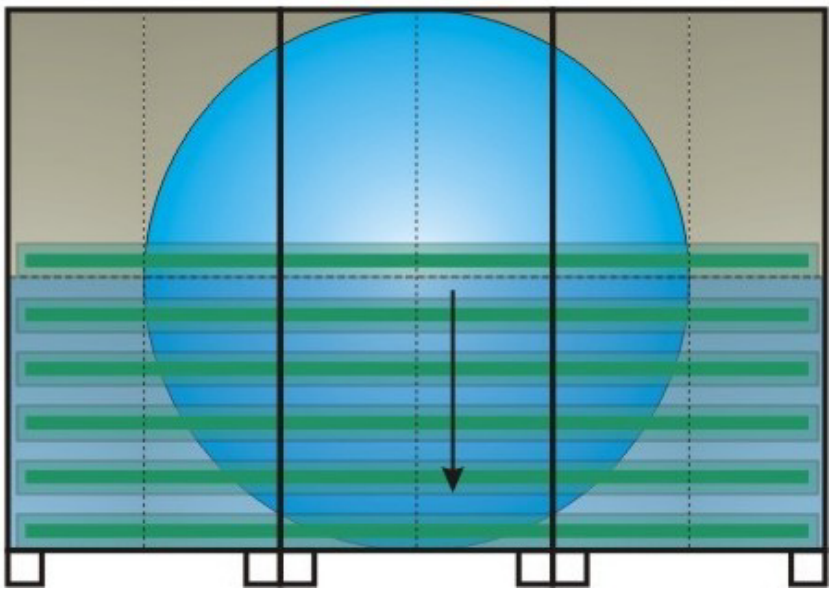

Figure 8: The RSS detector consists of three mosaiced 2K × 4K CCDs. The 8 arcmin diameter science field of view is shown as the central circle. In high-speed mode a slot only allows a restricted number of CCD rows to be illuminated, just above the frame transfer boundary. Following an exposure, the CCD rows are clocked down by twice as many rows as the width of the slot, and eventually readout by the 6 serial readout registers simultaneously. In this example a slot of ~204 pixels (~27 arcsec) width is depicted, each one shifted down by 408 pixels after each exposure.

6.2 Grating Spectroscopy

A slit-mask mechanism at the SALT focal plane allows for long-slit and, taking advantage of the large SALT field, multi-slit (up to 100) observations. Dispersers include a complement of volume phase holographic (VPH) gratings RSS designed to cover a wide wavelength range (320 – 900 nm), with an upgrade path for a near-infrared arm (850 nm – 1.7 microns), which would share the collimator optics with the visible beam. This required the use of NaCl lenses, for good imaging and color correction over such a broad wavelength range. CaF_2 and fused silica were the only other materials used in the design. The beam diameter was 150 mm and allowed for a maximum resolving power of R = 5500 for a filled 1.2 arcsecond slit. Higher resolving powers are possible with narrower slits, and thus lower slit throughput, with a practical maximum, limited by the internal image quality of the spectrograph and acceptable slit-loss, of ~13,000 for a 0.5 arcsecond slit.

RSS has a complement of five volume phase holographic (VPH) gratings and one transmission grating, all available at any time. The gratings were chosen to provide spectroscopic capability over the entire wavelength range of the detector and resolutions from R~500 to R~5500. VPH gratings have high diffractive efficiency and significantly reduced scattered light (as well as other benefits) as compared to standard surface-relief gratings[17]. Also, VPH gratings can be tuned to shift the diffraction efficiency peak to a desired wavelength. The use of such gratings requires the camera to be able to articulate, to accommodate various grating tilts. The inserted grating resides on a rotation stage, and the entire camera articulates about the same axis as the grating rotation, so that the grating is used in a Littrow configuration, where VPH gratings are most efficient.

The five VPH gratings chosen have groove densities of 900, 1300, 1800, 2300 and 3000 lines/mm, with peak efficiencies at 600, 570, 620, 520, and 370 nm, respectively. The surface relief grating is a 300 lines/mm grating and was added primarily as a survey grating for large wavelength coverage over a large field of view when used with multi-slit masks. A traditional transmission grating was chosen over a VPH grating in this regime due to the extremely large blaze shift and poor efficiency at large off-axis angles for VPH gratings. Also, VPH gratings have lower peak efficiency than traditional gratings at such low groove densities.

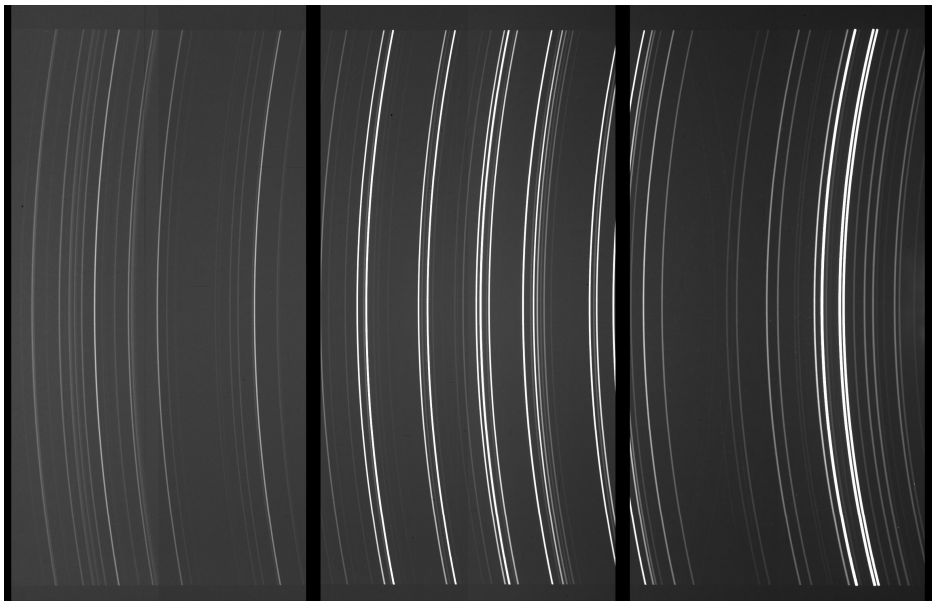

Figure 9: A spectrum of a calibration lamp through a 1.2 arcsecond long-slit, with the camera articulation at maximum. The curvature of the lines is caused by the variation of blaze wavelength with field angle, i.e. the dependence of beta (the diffracted angle) on gamma (the input angle perpendicular to the dispersion direction) in the grating equation.

Since its installation on the telescope in October 2005, RSS has been undergoing commissioning tests, initially concentrating on long-slit spectroscopy. Other modes will be commissioned as full functionality of the telescope, and particularly the prime focus payload, which contains crucial supporting subsystems, like the calibration system, atmospheric dispersion compensator (ADC)[18] and moving exit pupil baffles, is achieved. Multi-object spectroscopy (MOS) will not be attempted until the ADC is commissioned, and a fully functional Telescope Control System allows for the alignment of the laser cut slits masks on-sky.

Some Commissioning and Performance Verification observations of RSS in long-slit spectroscopy mode have been obtained, and the following figures are some examples of recently obtained data.

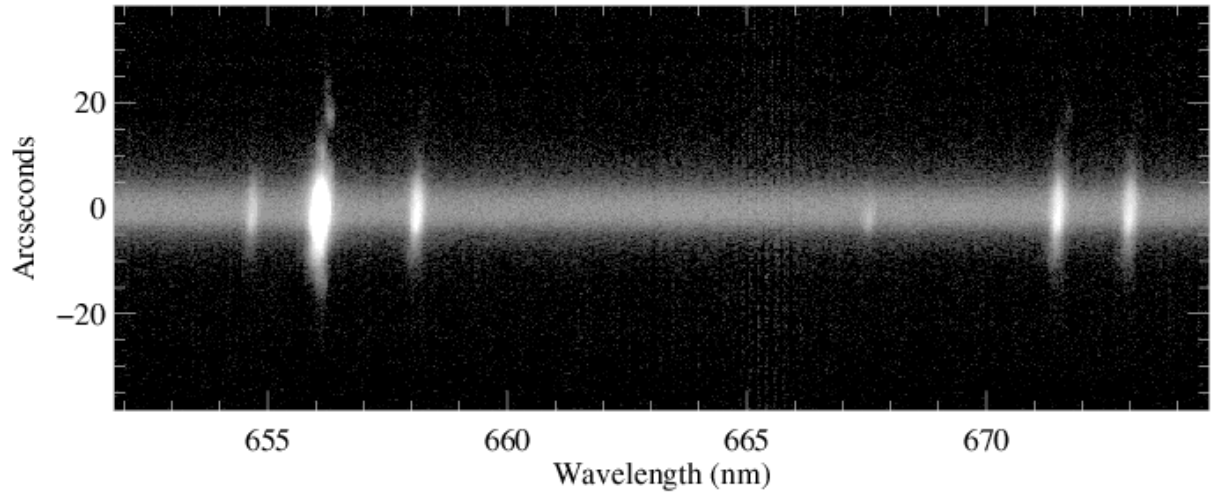

Figure 10 shows a long-slit spectrum of the star-bursting dwarf galaxy NGC 1140 in the region of Hα at the highest resolving power configuration of RSS[19]. These data have been background subtracted and corrected for the wavelength shift from the systemic velocity of the galaxy. The data were taken during the early commissioning phase of the spectrograph.

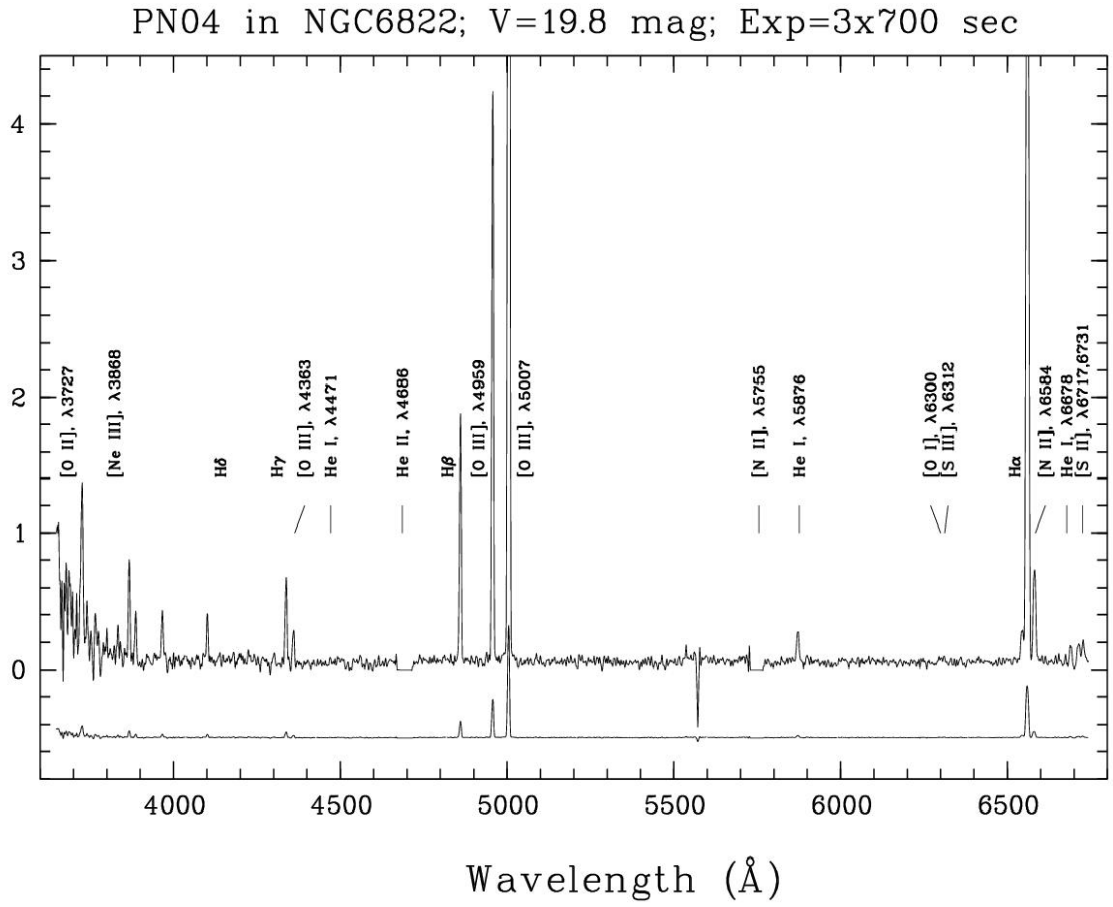

Figure 11: A recent RSS long-slit observation of a V~20 Planetary Nebula in the nearby galaxy NGC6822. The oxygen, neon and nitrogen abundances were calculated with accuracy ~0.1-0.15 dex using this spectrum.

6.3 Fabry-Perot Imaging Spectroscopy

Fabry-Perot (F-P) imaging spectroscopy with RSS over the full 8 arc minute field of view forms one of the core capabilities of SALT and will enable observations of both absorption and emission line sources of varying extent in five resolving power regimes. The sensitivity to extended diffuse emission is afforded by the large collecting area of a F-P spectrograph on SALT, enabling the mapping of velocity structure and line strength and shape. The ability to both simultaneously detect and observe emission lines, for example in galaxy clusters or halos, is one advantage of the F-P mode. Coupling the RSS polarimetric and F-P modes will provide a unique capability for imaging spectropolarimetry. Details of the RSS F-P design have been discussed before[11], so here we present an update on the actual measured lab performance of the completed F-P system, which has still to be commissioned on-sky.

The F-P system consists of three 150 mm aperture etalons, each covering the 430 – 900 nm spectral region, which can be run in dual etalon mode. The plate spacing of the etalons is 5, 28, and 135 microns, respectively; larger spacings produce higher resolving power. The etalons can be tuned to any wavelength within this range with piezoelectric actuators that vary the spacing and parallelism of the etalon plates. Capacitors sense the relative plate positions, and a servo control system maintains the spacing and parallelism. Forty interference filters select the desired F-P order.

Figure 12 shows the measured spectral resolution of the system over its wavelength range. Lowest resolution is obtained by imaging through the filters alone, with no etalons inserted. Since the piezo actuators have enough range to change the gap of the lowest resolution etalon by about a factor of two, two resolution modes (TF and LR) are produced using the low resolution etalon and a filter. The higher resolution modes (MR and HR) are produced in dual etalon mode by using one of the higher resolution etalons in series with the low resolution etalon and a filter, tuning both etalons to the same wavelength. The measured transmission of the filters and etalons are shown in Figure 13.

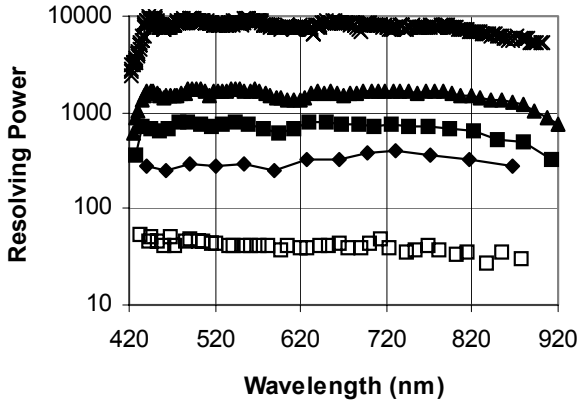

Figure 12: The RSS-FP Spectral Resolutions. Open Squares: interference filters; Diamonds: TF mode; Filled Squares: LR mode; Triangles: MR mode; X: HR mode.

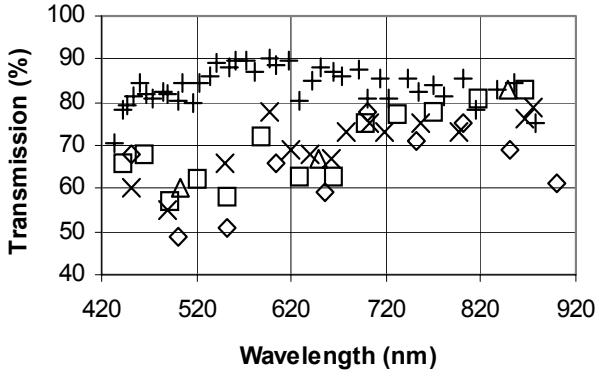

Figure 13: RSS-FP system efficiencies. Plus symbols: interference filters; Squares: TF mode; Triangles: LR mode; X symbols: MR mode; Diamonds: HR mode

Figure 14 demonstrates the effect of combining two etalons in the HR mode. The entrance aperture of the RSS was uniformly illuminated with a neon lamp. The transmission wavelength varies over the field, since the etalons are located in a collimated beam. Thus rings of bright illumination are produced at a radius where the transmitted wavelength matches one of the lamp spectral lines.

Figure 14a shows the LR mode, with the 651.6 nm filter (of FWHM 15.6 nm), the low resolution etalon tuned to a central wavelength of 651.8 nm, and the 650.7 nm neon line appearing as a moderate sized ring. Figure 14b shows the transmission of the high resolution etalon combined with the same filter. The pattern is complicated by two effects: there are four strong neon lines that pass through the filter, and the free spectral range of the etalon is 1.6 nm and the wavelength gradient from the center to the edge of the field is 2.1 nm, so the same line can appear in successive orders at different field angles. Figure 14c shows the full dual-etalon HR mode image, with the low resolution etalon selecting the desired order of the high resolution etalon, and the filter selecting the desired order of the low resolution etalon. Only the 650.7 neon line appears.

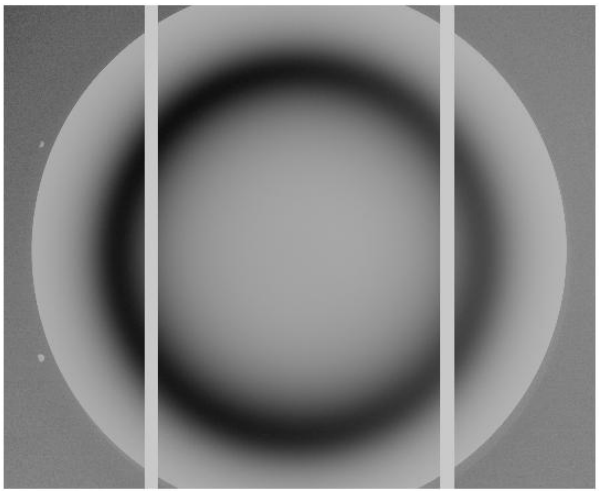

Figure 14a: F-P arc emission line rings for Low Resolution etalon tuned to 650.7nm neon line, with 15.6 nm wide (FWHM) narrow band filter.

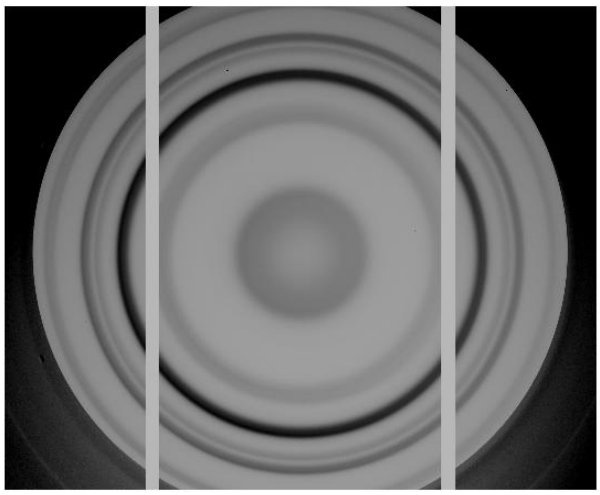

Figure 14b: Same as fig. 14a, but with the High Resolution etalon and same filter. Multiple rings arise from different lines falling within the filter bandpass.

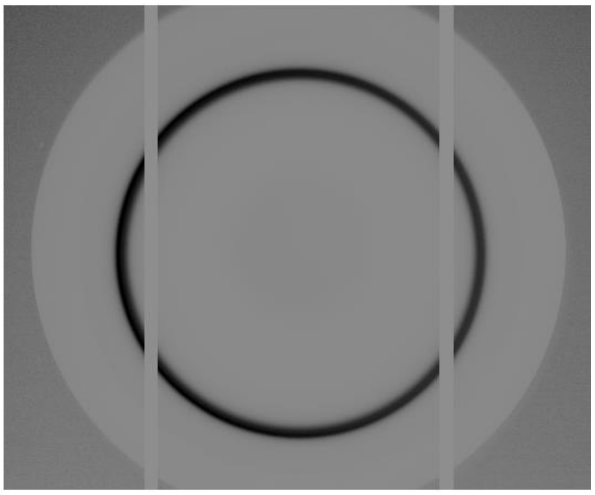

Figure 14c: 670.7 nm neon ring from dual etalon operation.

Figure 14: Neon calibration lamp exposures with 651.6 nm filter, etalons tuned to 651.8 nm central wavelength. (a) Low resolution etalon alone, 650.7 nm line. (b) High resolution etalon alone, multiple lines and orders. (c) Low and high resolution etalons, 650.7 nm line selected.

6.4 Polarimetry modes

The design and capability of the RSS polarimetric modes have been discussed previously[16]. The optics utilize a "wide-field" design, employing a polarizing mosaic beam-splitter in the collimated beam, just after the etalons, which takes the central half of the field and splits it into two orthogonally polarized fields: the "ordinary" (O) and "extraordinary" (E) beams. A polarization modulator, either or both a ½λ and ¼λ waveplate, is inserted just after the focal plane, which modulates the polarization state with time by rotating the waveplates. The difference between the intensities of the O and E images as a function of time yields the linear and/or circular polarization.

The beamsplitter, a 3 × 3 array of calcite Wollaston prisms, may be inserted just before the first camera element in the collimated beam. This ensures that there is no vignetting of the split beam by the dispersers, especially the Fabry-Perot etalons, which would compromise the polarimetric precision. Also, by placing the beamsplitter after the etalons, both the E and O fields have the same wavelength gradient in Fabry-Perot mode, enabling direct differencing of the two fields. One interesting characteristic of the Wollaston prisms, which can be exploited to produce a unique observing mode, is their intrinsic chromatic dispersion. Without filters or dispersers, the O- and E- images will be dispersed by the beamsplitter prisms into short spectra, perpendicular to the usual spectral dispersion direction. This provides a very low resolution (R ~ 50) spectropolarimetric imaging mode (like objective prism spectroscopy) over the 4 × 7.2 arcmin field.

Clocking of the CCD, as described in §6.1 for high-speed spectroscopy, will allow for high time resolution imaging linear or circular polarimetry. In this mode the beamsplitter will be rotated 90º, so that the O- and E-images of the object of interest would be aligned with the slot. Thus pairs of images, corresponding to the two different polarization states, can be read out very rapidly.

The modulator consists of the two rotating superachromatic waveplates near the beam “waist” in the collimator. This position was chosen because it minimizes the waveplate size and cost. The first waveplate is a 105 mm diameter half-wave plate, for linear spectropolarimetry covering a 4 × 7.2 arcmin field of view. The 60 mm quarter-wave plate can also be inserted, providing a 3.0 arcmin diameter unvignetted field for circular, or all-Stokes, polarimetry. The modulator is thus placed ahead of any optical elements with polarization sensitivity, like the fold mirror and the dispersors. Spectropolarimetric modes with RSS are possible through insertion of dispersers, either gratings or etalons. Synchronization of the waveplate rotation with on-chip charge shuffling will allow for accurate simultaneous measurements of all the Stokes parameters from time series spectropolarimetry.

The right panel of Figure 15 shows a low dispersion spectropolarimetric image of a continuum lamp taken through a series of slitlets and an HN32 polaroid. The field of view for polarimetric modes will be limited in the Y-direction to half the field (4 arcminutes; see left panel of Figure 15 – spectra taken without the beamsplitter) to allow for the clean separation of the "E" (upper half) and "O" (lower half) spectra on the detector. The polarization signal is derived from (E-O)/(E+O); this differential method cancels out the deleterious effects of variable atmospheric transparency. In this case one can see that the continuum light is polarized for wavelengths below 700 nm (chips 1 and 2, left and centre) and becomes unpolarized in the near infrared (chip 3; right).

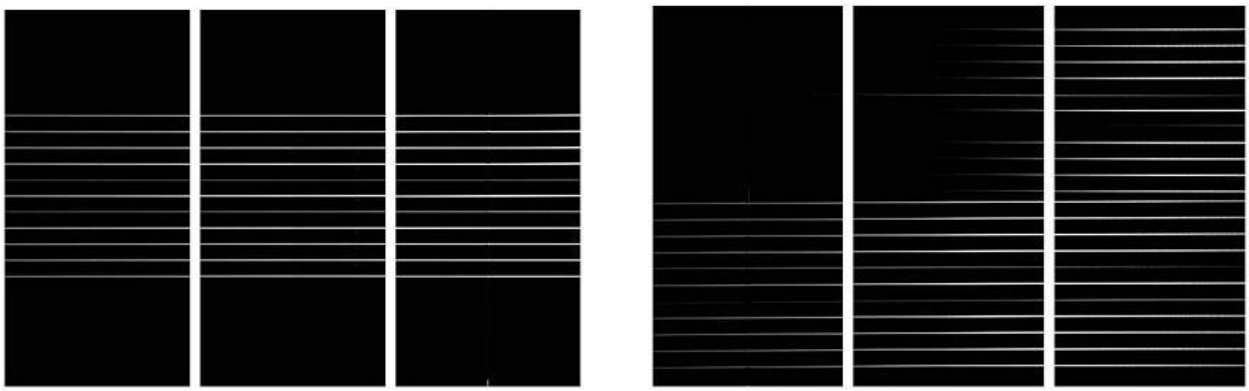

Figure 15: Laboratory tests of the RSS linear spectropolarimetry mode. Left is normal spectroscopy mode (no beamsplitter), right is after the beamsplitter and a Polaroid were inserted, producing a polarized signal in the left two CCDs, but none in the right CCD, due to the non-polarizing properties of the HN32 polaroid at longer wavelengths.

7. SALTHRS: HIGH RESOLUTION SPECTROGRAPH

The third First Generation instrument, the SALT High Resolution Spectrograph (SALTHRS)[11], suffered delays in development due to both technical issues and lack of full funding. This has resulted in a significant delay in its development, with the final design only being completed in April 2005. The SALTHRS design is for a dual-beam fibre-fed white-pupil R4 échelle spectrograph, employing VPH gratings as cross dispersers. The cameras are all-refractive. The concept is for SALTHRS to be an efficient single object spectrograph using pairs of large 300μm to 500μm (1.3-2.2") diameter optical fibers, one for source (star) and one for background (sky). Some of these will feed image slicers, allowing for up to 3 slices in the spatial direction, before injection into the spectrograph, which will deliver a resolving power of between R =17,000 (un-sliced 500μm fibers) and 70,000 (sliced 350μm fibers). The wavelength coverage of the two beams, split by a dichroic, will be in the region 370-560 nm (blue) and 560-870 nm (red). A single 2K × 4K CCD will be sufficient to capture all the blue orders, while a 4K × 4K detector will be required for the red. Complete free spectral ranges are covered.

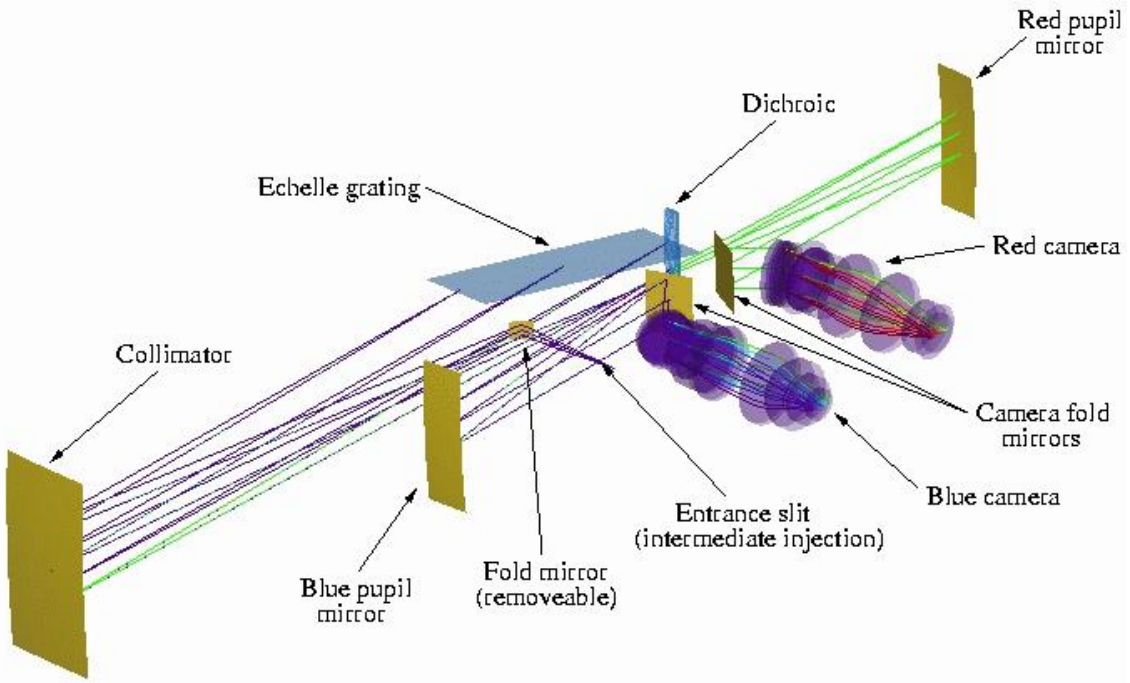

Figure 16: Layout of the proposed SALT HRS, which is a fiber-fed dual-beam white-pupil R4 échelle spectrograph.

The spectrograph will be enclosed in a vacuum tank to improve stability of the instrument, and to ensure the optics remain in a pristine condition. In addition, to allow for precise measurement of radial velocities, various additional techniques may be applied (e.g. use of an iodine absorption cell, externally dispersive interferometry (EDI) or simultaneous injection of ThAr arc spectra). To ensure accurate background subtraction, both beam switching and "nod & shuffle" techniques will be supported by HRS and the Fiber Instrument Feed, mounted on the Prime Focus Payload.

The final design of SALTHRS was completed by the University of Canterbury, New Zealand, a SALT partner, with Prof. Peter Cottrell as the Principal Investigator and Dr Michael Albrow as Instrument Scientist. At the time of writing, a general RFP has been issued for the construction of SALTHRS, which has an estimated construction cost of ~$2.2M.

8. INSTRUMENT COMMISSIONING EXPERIENCE

While the telescope and subsystems were designed, contracted and managed by the SALT Project Team, the first-light instruments were built by consortium partners whose Principal Investigators (PIs) were responsible for the overall management. Monthly technical and quarterly management, budget and schedule reports were sent to the SALT Project Scientist, who had overall responsibility for the instruments. Instrument review meetings were called for by the Project Scientist, who appointed external reviewers who met with representatives of the SALT Science Working Group and Instrument Teams.

As might be expected with one-off science instrument projects, despite the best attempts at defining realistic schedules, these inevitably slipped. The inter-connection of various tasks, and the consequences of delays in different subsystems, were difficult to predict. In hindsight it is clear that at least in the case of RSS, additional personnel may have alleviated these schedule pressures. For both instruments a delay of ~1 year was experienced in final delivery, although due to telescope delays of a similar amount, this did not have as significant an impact as it might have.

It also became clear after installation on the telescope that the acceptance tests conducted in the laboratory were not always adequate to test the instruments in the real telescope environment (e.g. temperature extremes). Although jigs were set up to test the instruments at the different nominal gravity vectors, it became clear that these were insufficient to test for all the degrees of freedom, particularly instrument rotation on an inclined plane. Mechanisms on SALTICAM failed early on due to both of these effects, and although temporary measures were employed to address them, some re-design has also been necessary. Similarly for RSS, the most complex mechanism, used to exchange focal plane slit masks from a "juke box", ran into alignment problems, and has had to be redesigned.

On a positive note, however, both first-light instruments are now operational and some science data is being obtained as part of the on-going commissioning process. Finally, in terms of final costs the two instruments, SALTICAM and RSS were, respectively within 5% and 9% of their original baseline cost estimates defined at PDR, namely $0.564M and $4.374M respectively, which included risk provision (15% and 20% respectively).

9. SUMMARY

This paper has described the designed capabilities the SALT First Generation instruments, which are targeted at the strengths of the SALT design, and particularly its enhanced capabilities: UV/blue efficiency, field of view, image quality, rare instrument modes and rapid instrument configurability. The "first-light" instruments, SALTICAM and RSS, were installed on SALT in mid- to late-2005, and they are now in the middle of their commissioning and "performance verification" phases (as is the telescope itself), expected to extend until the end of 2006. Observations have already indicated the great promise of SALT and its instruments in delivering excellent scientific returns.

ACKNOWLEDGMENTS

The success of SALT, exemplified by the fact that it has only taken 5 years to move from ground-breaking to "first light", is due to a great many talented and committed people. These include members of the SALT Project and Operations Teams, staff at the SAAO, the numerous personnel at our SALT partners working on the first generation instruments and the members of the SALT Board and Science Working Group. To all of those who have contributed so much, we give our sincere thanks. We also acknowledge the assistance and advice of other telescope and instrument makers, particularly our friends and colleagues at the Hobby Eberly Telescope, and the external reviewers who so gladly gave of their time to help ensure we had an excellent telescope and suite of instruments: Eli Atad-Ettedgui, Sam Barden, Richard Bingham, John Booth, Bernard Delabre, Hans Dekker, Rodger Haynes, Gary Hill, Hilton Lewis, Phillip MacQueen, Steve Shectman, Keith Taylor, Dave Walker and Fred Watson, to name a few.

REFERENCES

1. R. Stobie, K. Meiring, D. Buckley, "Design of the South African Large Telescope (SALT)", in *Optical Design, Materials, Fabrication, and Maintenance*, P. Dierickx, ed., *Proc. SPIE* **4003**, pp. 355-362, 2000.
2. D.A.H. Buckley, "The Southern African Large Telescope: an alternative paradigm for an 8-m class telescope", *New Ast. Rev.*, **45**, pp.13-16, 2001.
3. J. G. Meiring, D.A.H. Buckley, M. Lomberg M. and R.S. Stobie, "The SALT project: progress and status after 2 years", in *Large Ground-based Telescopes*, J.M. Oschmann and L.M. Stepp, eds., *Proc. SPIE* **4837**, pp. 11-25, 2003.
4. J. G. Meiring and D.A.H. Buckley, "SALT Project: Progress and Status after Four Years", in *Large Ground Based Telescopes*, J.M and Oschmann, L.M. Stepp, ed., *Proc. SPIE* **5489**, pp. 592-602, 2004.
5. T. A Sebring and L. W. Ramsey, "The Hobby-Eberly Telescope: A progress report", in *Optical Telescopes of Today and Tomorrow*, A. L. Ardeberg, *Proc SPIE* **2871**, pp. 32-37, 1997.
6. L. W. Ramsey, et al., "The early performance and present status of the Hobby-Eberly telescope", in *Advanced Technology Optical/IR Telescopes VI*, L. M. Stepp, ed., *Proc. SPIE* 3352, pp. 34-42, 1998.
7. D. O'Donoghue and A. Swat, "The Spherical Aberration Corrector for the SALT", in *Large Lenses and Prisms*, R.G. Bingham and D.D. Walker, eds., *Proc. SPIE* **4411**, pp. 72-78, 2001.
8. J. Wolfe, D. Sanders, S. Bryan and N. Thomas, "Deposition of durable wide-band silver mirror coatings using long-throw, low-pressure, DC-pulsed magnetron sputtering", in *Specialized Optical Developments in Astronomy,* E. Atad-Ettedgui and S. D'Odorico, eds., *Proc. SPIE* **4842**, pp.343-351, 2003.
9. D. A. H. Buckley, and D. O'Donoghue, N. J. Sessions and K. H. Nordsieck, "Instrumentation Options for the Southern African Large Telescope (SALT)", in *Optical and IR Telescope Instrumentation and Detectors*, M. Iye and A. F. Moorwood, eds., *Proc. SPIE* **4008**, pp. 72-82, 2000.
10. D. A. H. Buckley, J. B. Hearnshaw, K. H. Nordsieck and D. O'Donoghue, "Science drivers and first generation instrumentation for SALT", in *Discoveries and Research Prospects from 6- to 10-meter class Telescopes II,* P. Guhathakurta, ed., *Proc. SPIE* **4834**, pp. 264-275, 2003.
11. D. A. H. Buckley, P.L. Cottrell, K.H. Nordsieck, D. O'Donoghue and T.B. Williams, "The First Generation Instruments for the Southern African Large Telescope (SALT)", in *Ground-based Instrumentation for Astronomy*, A. F. Moorwood,and M. Iye, eds., *Proc. SPIE* **5492**, pp. 6-74, 2004
12. D. O'Donoghue, et al., "SALTICAM: a $0.5M acquisition Camera: Every Big Telescope Should Have One", in *Instrument Design and Performance for Optical/Infrared Ground-based Telescopes*, M. Iye and A.F. Moorwood, eds., *Proc. SPIE* **4841**, pp. 465-476, 2003.
13. D. O'Donoghue, et al., "High-speed SALT instrument CCD detectors", in *Optical and Infrared Detectors for Astronomy*, J.D. Garnett and J.W. Beletic, eds., *Proc. SPIE* **5499**, pp. 406-413, 2004.
14. E. Burgh, et al., "The Prime Focus Imaging Spectrograph for the Southern African Large Telescope: optical design", in *Instrument Design and Performance for Optical/Infrared Ground-based Telescopes*, M. Iye and A.F. Moorwood, eds., *Proc. SPIE* **4841**, pp. 1463-1471, 2003.
15. H. A. Kobulnicky, et al., "The Prime Focus Imaging Spectrograph for the Southern African Large Telescope: operational modes", in *Instrument Design and Performance for Optical/Infrared Ground-based Telescopes*, M. Iye and A.F. Moorwood, eds., *Proc. SPIE* **4841**, pp. 1634-1644, 2003.
16. K. H. Nordsieck, K. P. Jaehnig, E. B. Burgh, H. A. Kobulnicky, J. W. Percival, and M. P. Smith, "Instrumentation for high-resolution spectropolarimetry in the visible and far-ultraviolet", in *Polarimetry in Astronomy*, S. Fineschi, ed., *Proc. SPIE* 4843, pp. 170-179, 2003.
17. S. C. Barden, J. A. Arns, W. S. Colburn, and J. B. Williams, "Volume-Phase Holographic Gratings and the Efficiency of Three Simple Volume-Phase Holgographic Gratings", *PASP*, **112**, 809, 2000.
18. D.O'Donoghue, "The Atmospheric Dispersion Corrector for SALT", in *Large Lenses and Prisms*, R.G. Bingham and D.G. Walker, eds., *Proc. SPIE* **4411**, pp. 79-84, 2001.
19. E. B. Burgh, J. S. Gallagher III, K. H. Nordsieck, J. W. Percival, M. P. Smith, D. O'Donoghue, D. A. H. Buckley, N. S. Loaring, "SALT/RSS Longslit Spectrosocopy of the NGC 1140 Starburst," American Astronomical Society Meeting, **208**, #14.03, 2006.